

## Gravitational Collapse of Uniform Spherical Gas Cloud

NINA FILIPPOVA,<sup>1</sup> MALIA KAO,<sup>1</sup> JOOHYUN LEE,<sup>1</sup> AND JACKSON WHITE<sup>1</sup>

<sup>1</sup>*Department of Astronomy, University Texas, Austin*

### 1. INTRODUCTION

Many astrophysical problems, such as star formation from molecular clouds, involve the gravitational collapse of cold, dense gas. In the simplest idealization, an isothermal, spherically-symmetric, uniform-density cloud will collapse to a singular point of infinite density within one freefall time (Truelove et al. 1998); the freefall time,  $t_{\text{ff}}$ , for such a cloud is

$$t_{\text{ff}} = \left( \frac{3\pi}{32G\rho_0} \right)^{1/2}. \quad (1)$$

In this case, the analytic solution for the time  $t_\rho$  it takes for the central density to reach a value of  $\rho$  is given by (Truelove et al. 1998)

$$\frac{t_\rho}{t_{\text{ff}}} = \frac{2}{\pi} \left[ \eta + \frac{1}{2} \sin(2\eta) \right], \quad (2)$$

where  $\eta$  is defined via

$$\cos(\eta) \equiv \left( \frac{\rho}{\rho_0} \right)^{-1/6}. \quad (3)$$

Because the gravitational collapse of a uniform, isothermal cloud has an analytic solution, it is an excellent test problem for hydrodynamical codes. However, realistic examples of gravitational collapse usually involve additional physics, such as various forms of heating/cooling, rotation, and magnetic fields. These phenomena introduce thermal pressure, rotational, and magnetic support, complicating the simple gravitational collapse of the cloud. Numerical simulations serve as an excellent tool for studying gravitational collapse in the presence of these additional forces – problems which may not have simple analytic solutions. In this work, we study the gravitational collapse of uniform-density spheres, beginning with the isothermal, gravity-only model, and progressively including realistic heating/cooling processes, solid-body rotation, and uniform ambient magnetic fields to the model, and compare the evolution of the central density of these models to the known analytic solution for isothermal collapse.

### 2. METHODS

We use the GIZMO code (Hopkins 2015) to solve the equations of (magneto)hydrodynamics for the gas throughout the collapse of each model. GIZMO is a flexible, massively-parallel, multi-physics simulation code. It introduces new Lagrangian Godunov-type methods for the solution of the (magneto)hydrodynamics equations, designed to combine many of the advantages of both Lagrangian smoothed-particle hydrodynamics (SPH) and Eulerian grid-based/adaptive mesh refinement

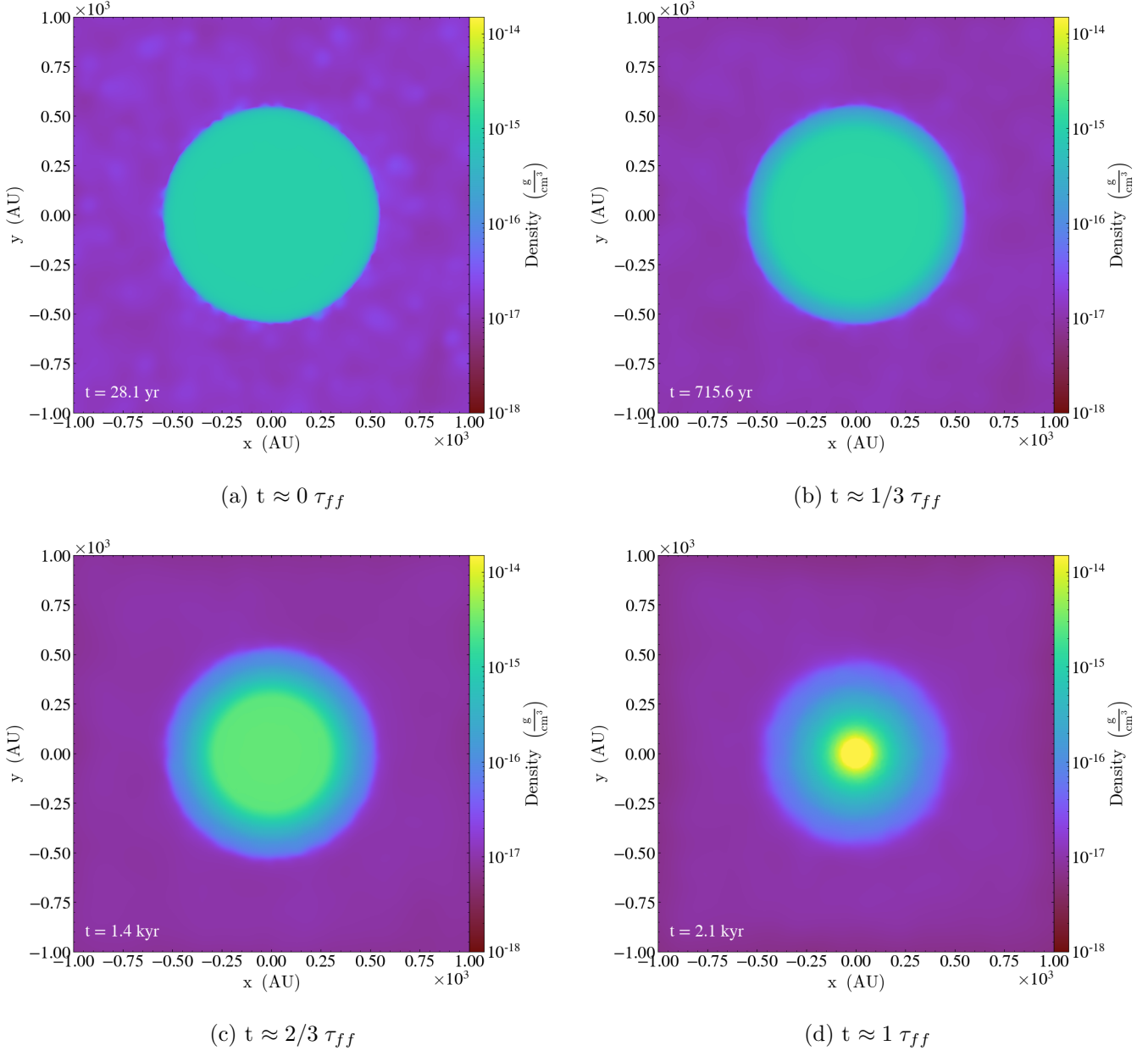


**Figure 1:** Density projection plots for static gas cloud collapse without heating/cooling or rotation.

(AMR) schemes through a moving, meshless particle distribution. These meshless-finite-mass/volume (MFM/MFV) schemes are automatically adaptive in resolution, and avoid the advection errors, angular momentum conservation errors, and excessive diffusion problems encountered with grid-based methods, while simultaneously avoiding the low-order errors inherent to SPH methods (Hopkins 2015). We used this novel MFM hydro solver for each run. Additional compile-time flags are used to enable additional physics, such as realistic heating/cooling (enabled by the ‘COOLING’ flag) and magnetohydrodynamics (MHD; enabled by the top-level ‘MAGNETIC’ flag).

Each model is initialized as a uniform sphere of gas of mass  $M = 1 M_\odot$  and radius  $R = 7.8 \times 10^{15}$  cm, corresponding to an initial density  $\rho_0 = 10^{-15} \text{ g cm}^{-3}$  and an initial freefall time  $t_{\text{ff}} = 2.1$  kyr.

The initial gas temperature is 10 K. The simulation volume is a box with side length  $L = 4R$ , with periodic boundary conditions; the remainder of the simulation volume is filled with a low-density ambient medium ( $\rho_{\text{ambient}} = 0.01\rho_0$ ). For the magnetized models, we also initialize a uniform magnetic field, oriented parallel to the  $z$ -axis. To initialize a uniform spherical gas cloud, we use the MAKECLOUD initial-conditions generating Python script (Grudić & Guszejnov 2021). MAKECLOUD establishes a gas cloud with a glass-like distribution, where the initial particle distribution is such that the system energy is minimized, ensuring there are no artificial discontinuities or shocks when the simulation begins. We modify the original MAKECLOUD Python script to enforce an initial density contrast of  $\rho_{\text{ambient}}/\rho_0 = 0.01$ . Each cloud consists of  $N = 10^5$  constant-mass gas particles, corresponding to a mass resolution of  $\Delta m = 10^{-5} M_\odot$ .

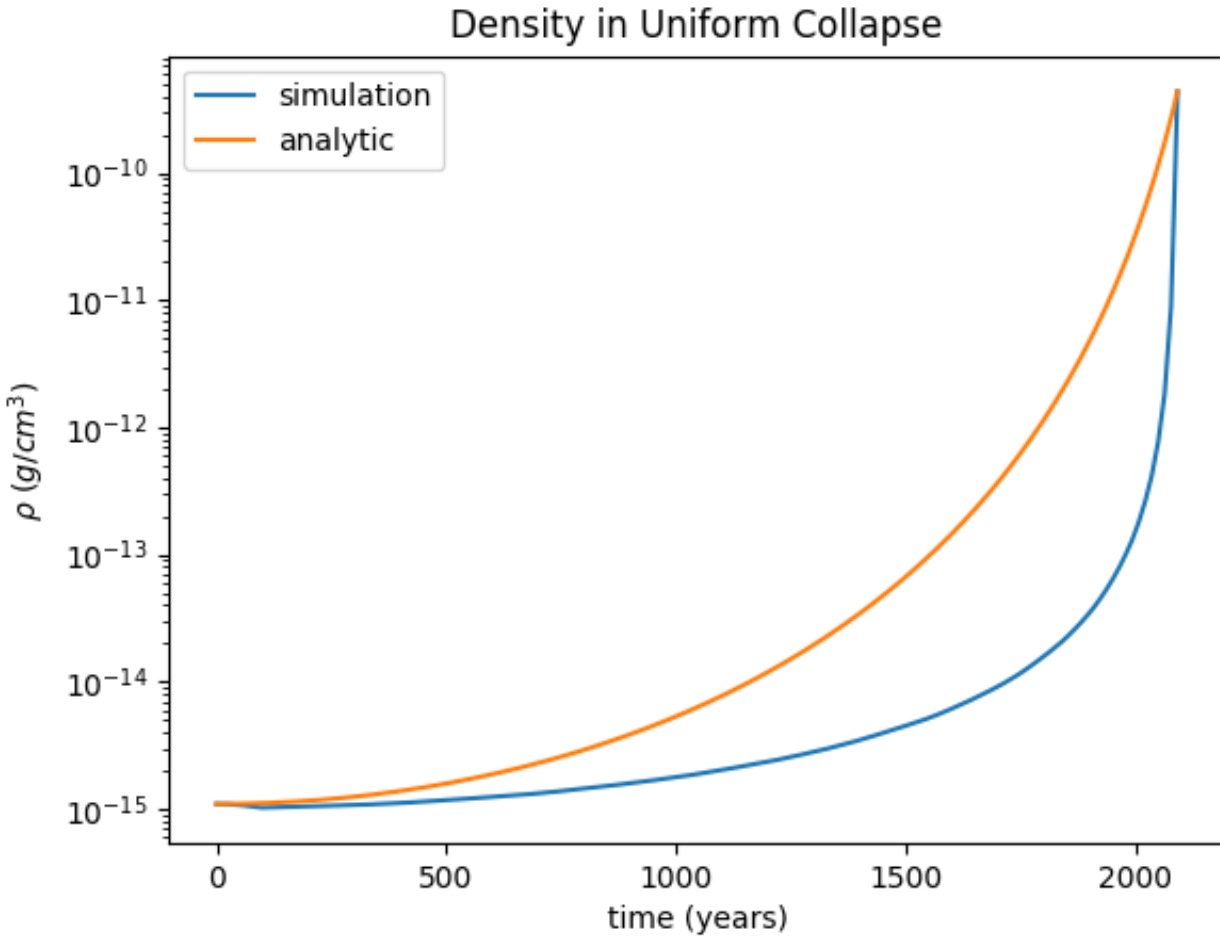


**Figure 2:** The analytic and numerical solutions match at the end time and are allowed to vary for the rest of the times. The densities from the simulation seem to match the analytic solution initially, but then diverge thereafter. This indicates that a model with isothermal, uniform collapse is not accurate in describing the change in maximum density throughout the collapse.

To run the calculations, we simultaneously use 24 cores on a single Knights-Landing (KNL) node on the STAMPEDE2 supercomputer at the Texas Advanced Computing Center (TACC). With this

parallelization, running a model with  $10^5$  gas particles takes only about 8 minutes to reach one freefall time.

### 3. RESULTS

#### 3.1. Static Isothermal Gas Cloud

The first simulation was run for a uniform, non-rotating gas cloud for a total simulation time of about one free-fall time ( $t_{ff} \approx 2.1$  kyr). The initial mass, radius, and temperature were again  $M = 1M_\odot$ ,  $R = 7.8 \times 10^{15}$  cm, and  $T = 10$  K respectively. The results from this simulation are shown in Fig. 1.

The equations in Section 3.2.1 in (Truelove et al. 1998) are used to compute the analytic solution for comparison with the solution from the simulation. The ratio  $t_\rho/t_{ff}$  in Eq. 2 was calculated using the maximum density in the last numerical calculation. The value  $t_{sing}$  given by

$$t_{sing} = \frac{t}{t_\rho/t_{ff}} \quad (4)$$

is the time of singularity in the numerical solution and was calculated using the result for  $t_\rho/t_{ff}$  from Eq. 2 and the time  $t$  associated with the last density calculation from the simulation. The analytic solution can then be calculated by numerically inverting

$$\frac{t_\rho}{t_{sing}} = \frac{2}{\pi} \left[ \eta + \frac{1}{2} \sin(2\eta) \right] \quad (5)$$

where the ratio  $t_\rho/t_{sing}$  is non-trivially related to the density. Eq. 5 is nearly identical to Eq. 2 except that the free-fall time is replaced by the time of singularity. This forces the analytic and

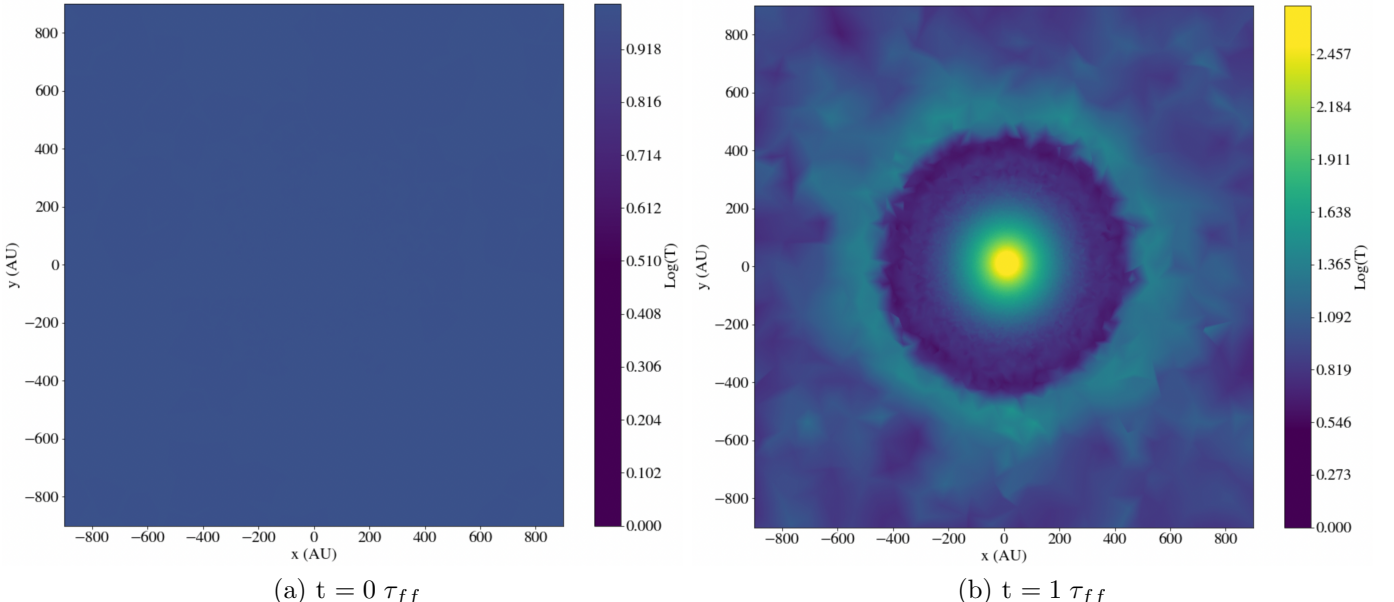


**Figure 3:** Temperature slice plots along the z-axis for static gas cloud collapse with realistic cooling/heating turned on. Early on, at  $t=0$ , the temperature is uniform as expected. At late times, around a single free fall timescale, the temperature rises substantially in the central core and partially in the outer edge of the star gas cloud.

numerical solutions to match at the end point, but allows them to vary before then (Truelove et al. 1998). This gives an indication of accuracy of the simulation as shown in Fig. 2.

### 3.2. Static Gas Cloud with Realistic Cooling/Heating

After rerunning the isothermal gas cloud with the ‘COOLING’ parameter turned on, the results changed substantially. Notably, the central density comparison with the analytic values given by Truelove et al. (1998), shown in figure 4, demonstrate almost perfect agreement. This is in stark contrast to the disagreement shown in section 3.1 with the static isothermal gas cloud case and illustrates the success of including the atomic and molecular processes included in the ‘COOLING’ function. The difference that arises from adding more accurate cooling/heating methods to the isothermal case is also evident in figure 3. While the gas cloud starts off as isothermal, it deviates significantly from this state and by the end of a single freefall time the central temperature is almost two orders of magnitude hotter than the initial isothermal temperature. Another interesting feature present in the temperature plot in figure 3 is the formation of an overly hot ring which appears to correlate with the outer edge of the collapsing gas cloud. This might suggest that a heating mechanism is present in the outer layers of the collapsing gas cloud, when the density quickly drops

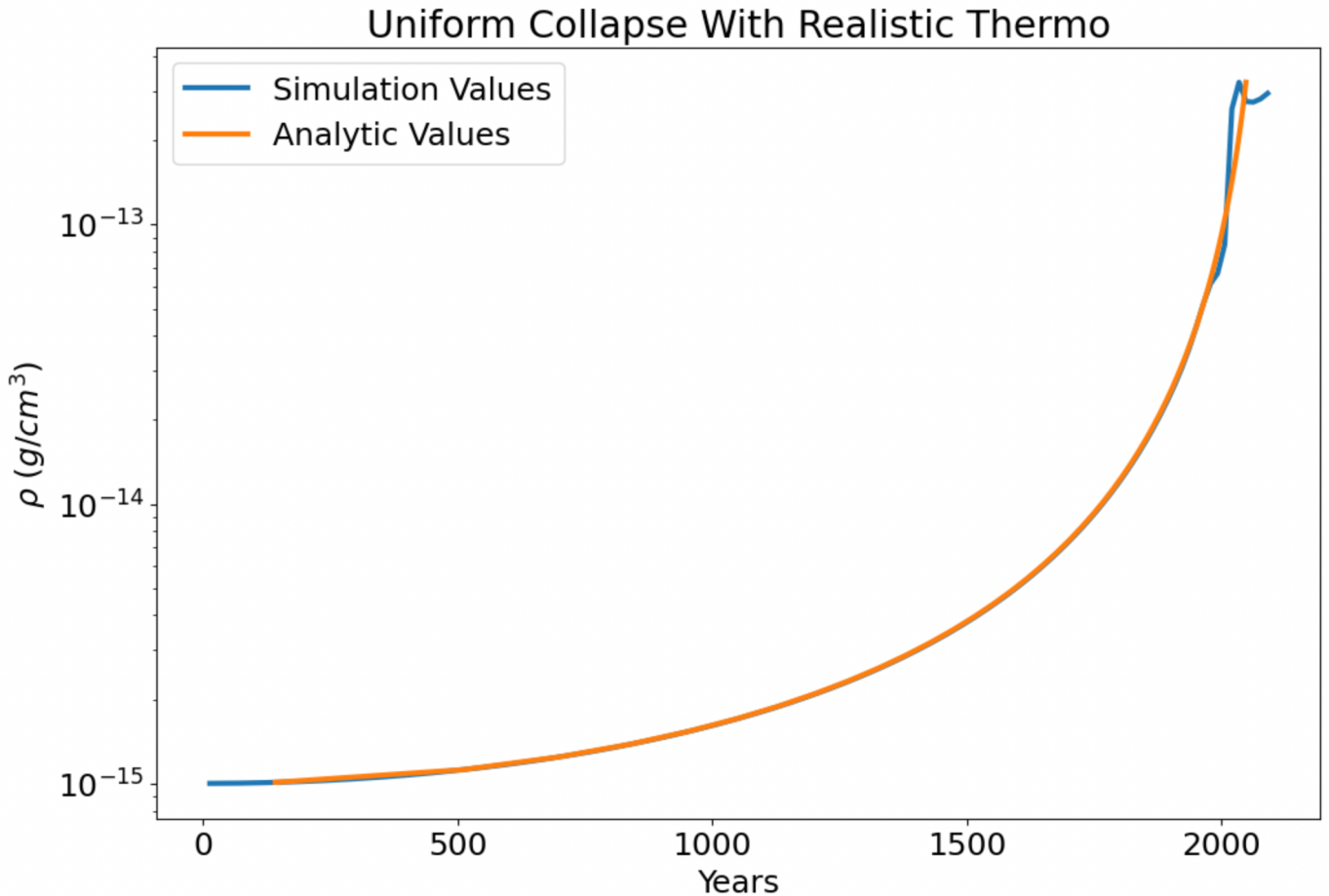


**Figure 4:** Central density comparison between analytic values calculated from Truelove et al. (1998) and simulated values calculated with GIZMO with the COOLING compile-time keyword turned on. The two curves almost exactly fit each other until around 1 free-fall time.

off, which is suppressed further inside the cloud. Or it could be a computational artifact that we failed to account for.

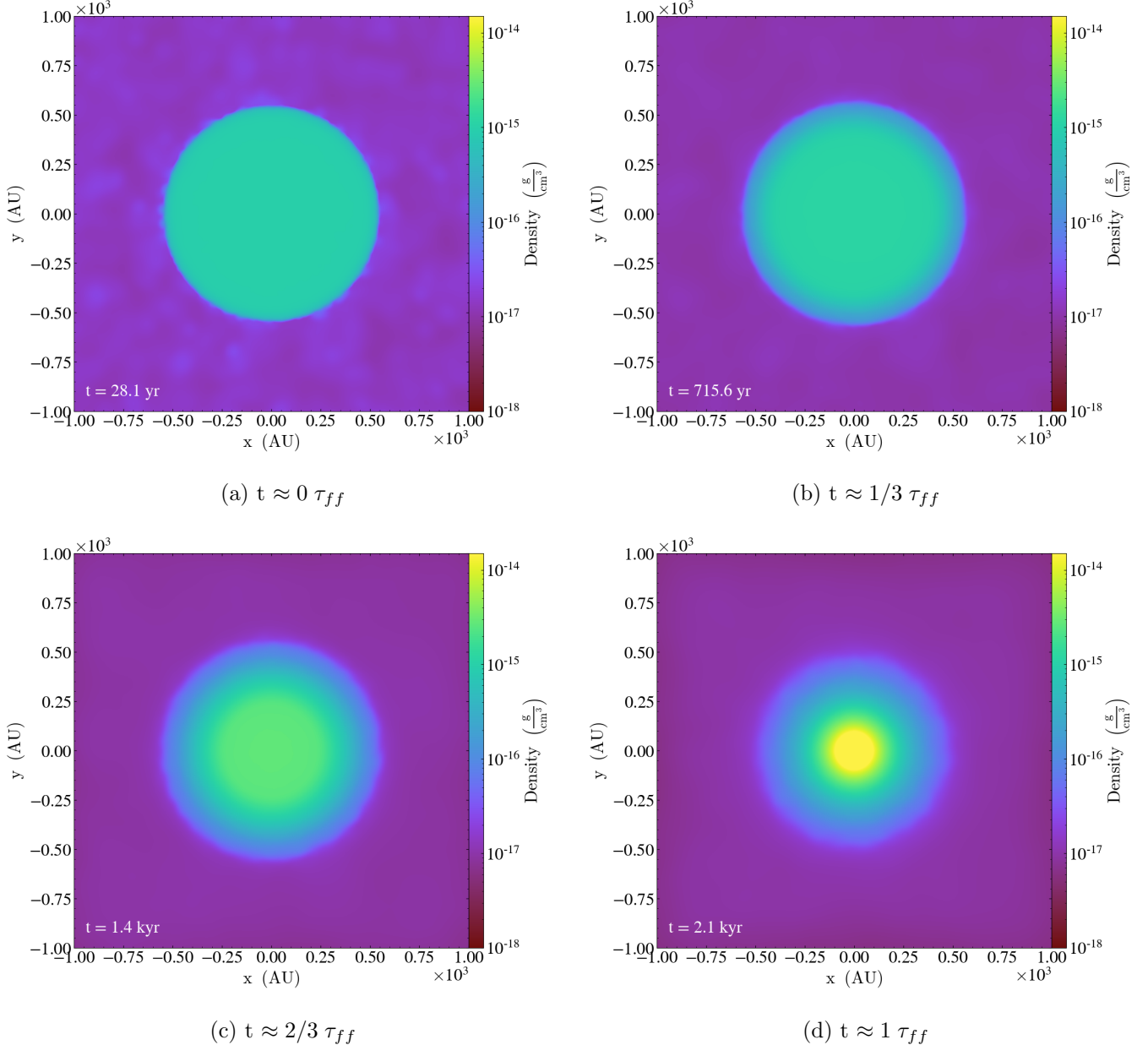


**Figure 5:** Density projection plots for static gas cloud collapse with realistic cooling/heating turned on.

The ‘COOLING’ flag considers a wide range of radiative cooling and heating methods that involve interactions between the gas particles in the cloud, such as hydrogen ionization and recombination, collisional, and free-free heating/cooling. For this simulation, many of these effects are only minimally present because most of the gas cloud is very cold ( $\lesssim 100\text{K}$ ) for the duration of a single free-fall time. Emitted radiation goes as  $T^4$  following the Stefan-Boltzmann law, so there will be very limited radiation emitted by the gas cloud over the initial thousand years. Most of the emitted radiation,

and resultant radiative cooling, will be generated in the core of the star over the last few hundreds of years of the simulation when the core reaches hotter temperatures. The cloud is also extremely diffuse (After 1 free fall time, the central core is still  $\sim 13$  orders of magnitude more diffuse than the optically thin solar photosphere), which makes it easier for emitted photons to escape as the mean free path goes as  $\rho^{-1}$ . However that also further reduces the impact of most of the cooling processes being considered. Many of the heating mechanisms considered, such as nuclear fusion, will also not happen on significant scales because the gas cloud is too disperse and cold at this stage. Most of the heating will come from the simple conversion of gravitational potential energy into kinetic/thermal energy through collisions that occur in the core.

### 3.3. Rotating Gas Cloud with Realistic Cooling/Heating

The rotating gas cloud simulations were carried out using GIZMO code with isothermal thermodynamics. The initialization of rotation velocities are done with MAKECLOUD. Since the code initializes rotation using rotation energy  $E_{\text{rot}}/E_{\text{grav}}$ , in order to initialize the cloud with a certain angular velocity, a simple calculation of the rotation energy ( $E_{\text{rot}}$ ) and gravitational energy ( $E_{\text{grav}}$ ) is needed. We employed Eq. 6 to perform the calculation.

$$|E_{\text{grav}}| = \frac{3}{5} \frac{GM^2}{R}, \quad E_{\text{rot}} = \frac{1}{5} MR^2 \Omega^2 \quad (6)$$

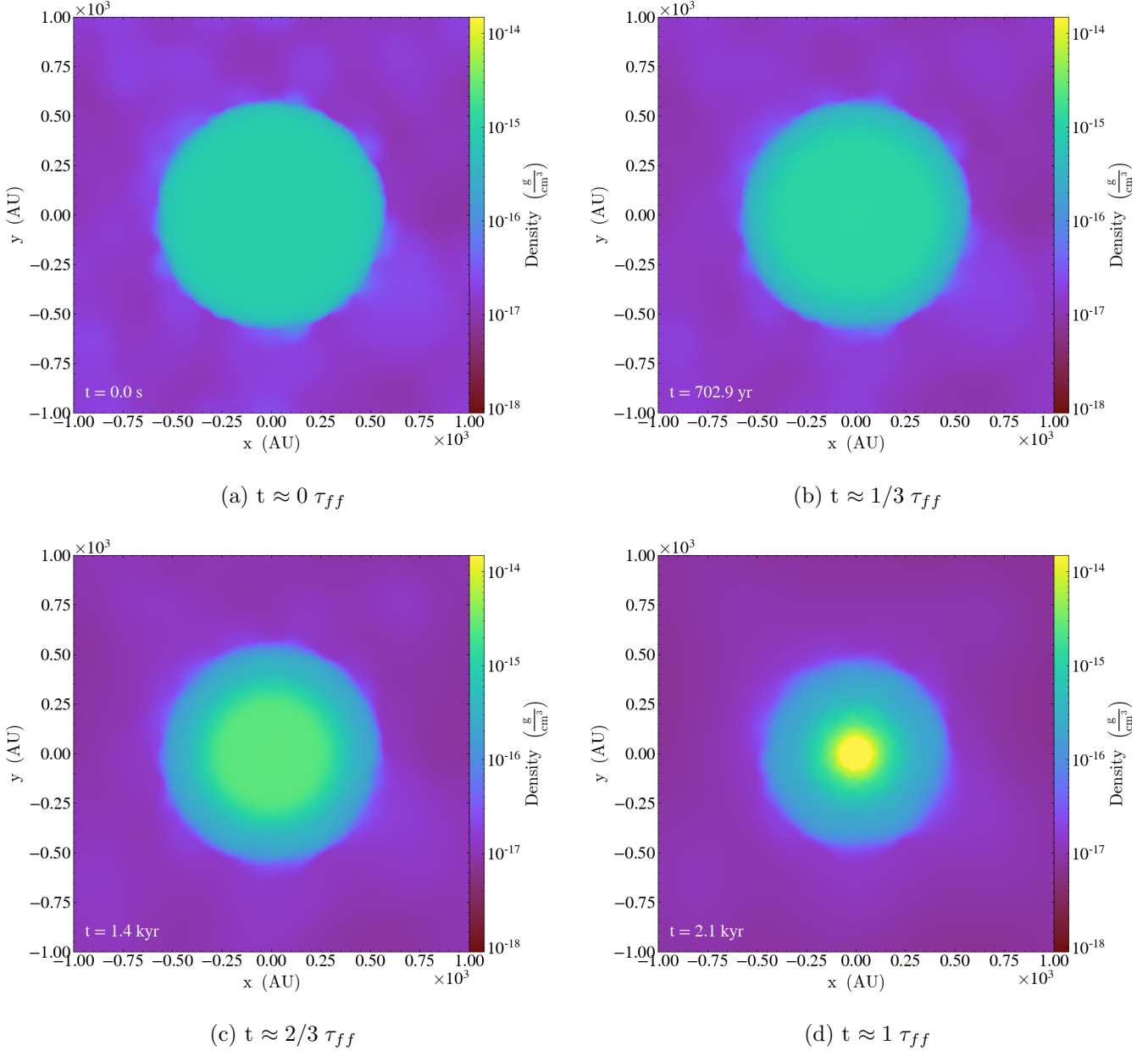
Firstly, a simulation with rotation velocities of  $\Omega = 10^{-12} \text{ s}^{-1}$  is initialized and run. Figure 6 shows four snapshots taken from the simulation. Qualitatively, the evolution of the rotating gas cloud does not look different from that of the static gas cloud which is presented in Figure 1. Next, simulations are initialized with rotation energy of  $E_{\text{rot}}/E_{\text{grav}} = 0.01, 0.1, 0.5$ . Figure 7 illustrates snapshots of those simulations at same time. Clearly, as the rotation energy gets larger, the collapse is prevented. The difference due to the rotation velocity is also shown in Figure 8 where we compare the analytic solution of the central density and our numerical results. Along with the simpleminded quantitative analysis with the snapshots, the variation from the analytic solution gets larger as the rotation gets faster. Especially in  $E_{\text{rot}}/E_{\text{grav}} = 0.5$  run, the gas cloud does not collapse, instead expands. This result is not surprising because the initial rotation velocity is too large for the outermost shell of the gas cloud to be bound by the gravitational potential energy. In fact, the factor of 0.5 corresponds to the kinetic energy of a virialized system, where the rotation should be rather Keplerian, not solid-like.

In terms of the angular momentum conservation of the GIZMO code, it turned out to perform very well. Figure 9 describes how the angular momentum changes with time, and the results show that the code conserves angular momentum within an accuracy of 1%. An interesting feature is that as collapse happens, the deviation from the initial angular momentum increases.

### 3.4. Magnetized Gas Cloud

The magnetized models were run with the GIZMO ‘COOLING’ and ‘MAGNETIC’ flags, enabling ideal MHD in addition to realistic heating/cooling. We varied the ratio of the initial magnetic to gravitational potential energy of the cloud, testing the values  $E_{\text{mag}}/E_{\text{grav}} = 0.01, 0.1$ , and 1.0, where

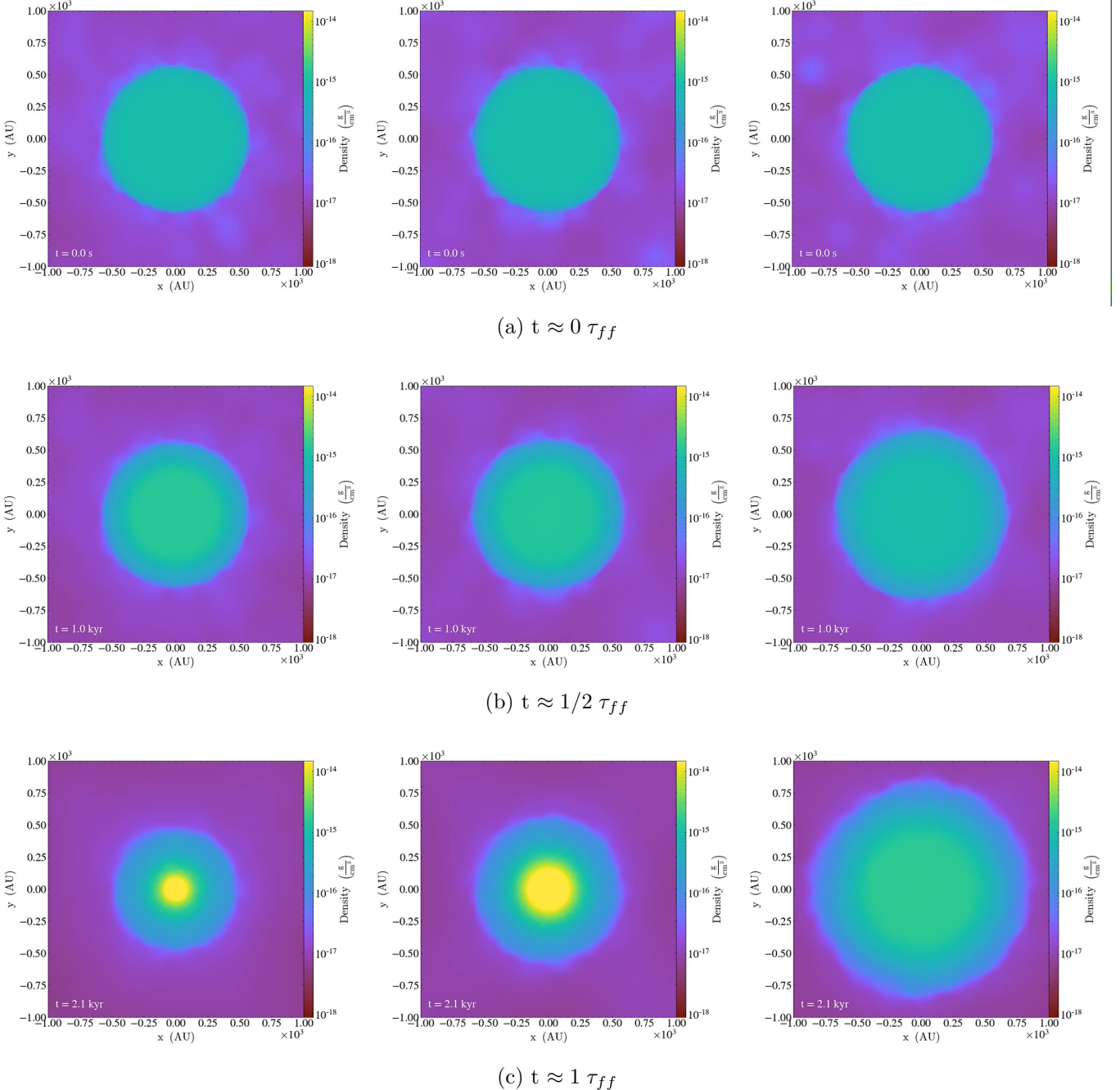
$$E_{\text{mag}} = \frac{1}{6} |B|^2 R^3 \quad (7)$$



**Figure 6:** Density projection plots for a gas cloud collapse with initial rotation velocities of  $\Omega = 10^{-12} \text{ s}^{-1}$  ( $E_{\text{rot}}/E_{\text{grav}} = 0.001192$ )

for a spherical, uniform-density cloud. The initially-uniform magnetic field is oriented along the  $z$ -axis in these simulations.

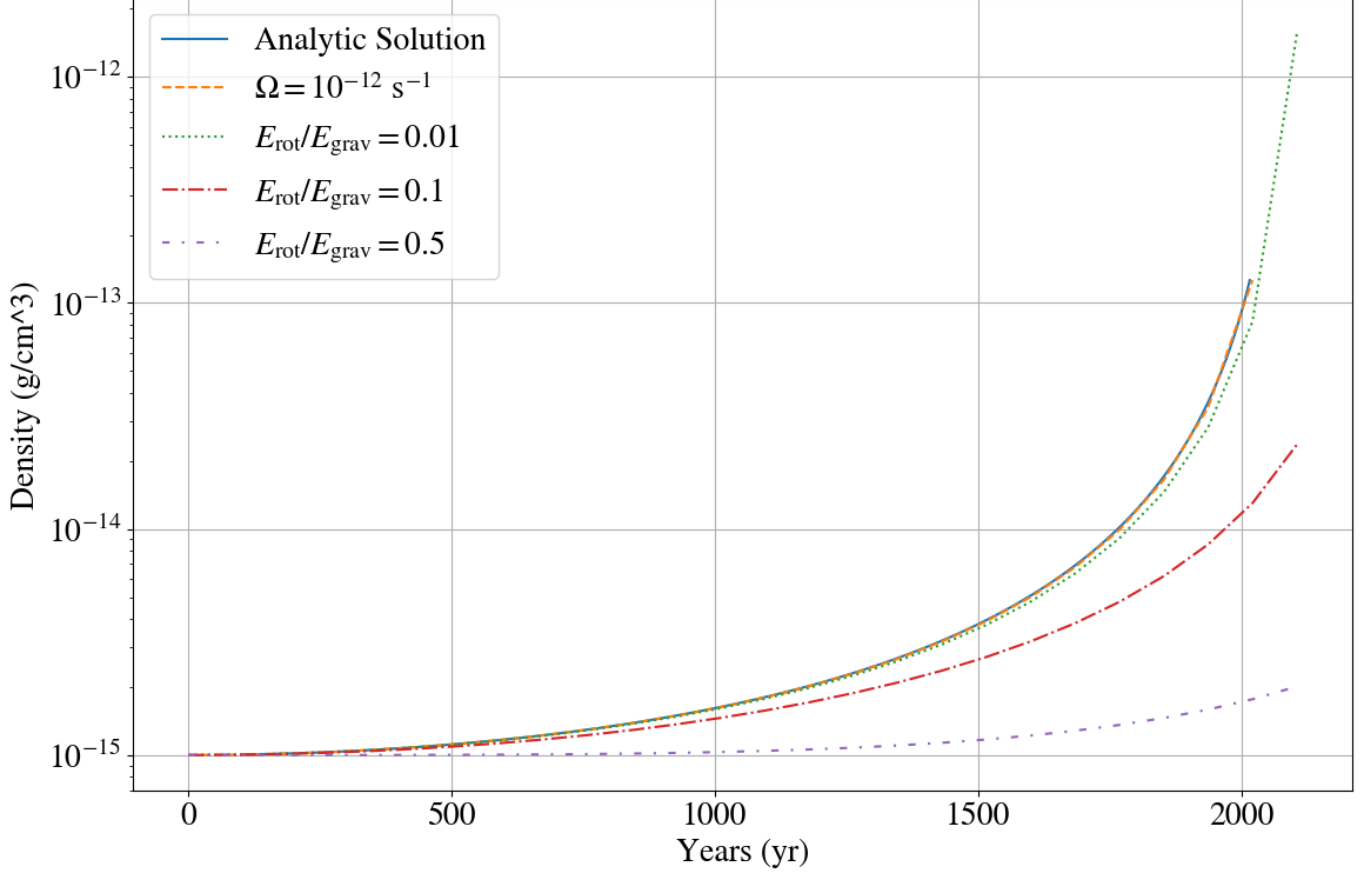
Due to the coupling between the magnetic field and the gas in the ideal-MHD approximation, adding a uniform magnetic field changes the problem from spherically-symmetric collapse to axisymmetric collapse. Magnetic pressure forces resist gravitational collapse perpendicular to the mean field direction; gas motion is preferentially oriented parallel to the magnetic field. Figure 10 shows snapshots of the projected gas density at  $t/t_{\text{ff}} = 0.5$  (top row) and  $t/t_{\text{ff}} = 1.0$  (bottom row), with the magnetic field strength in the models increasing from left to right across the columns. The initial



**Figure 7:** Density projection plots for a gas cloud collapse with initial rotation energy of  $E_{\text{rot}}/E_{\text{grav}} = 0.01$  (left column), 0.1 (middle column), 0.5 (right column). Faster the gas cloud rotates, harder it collapses.

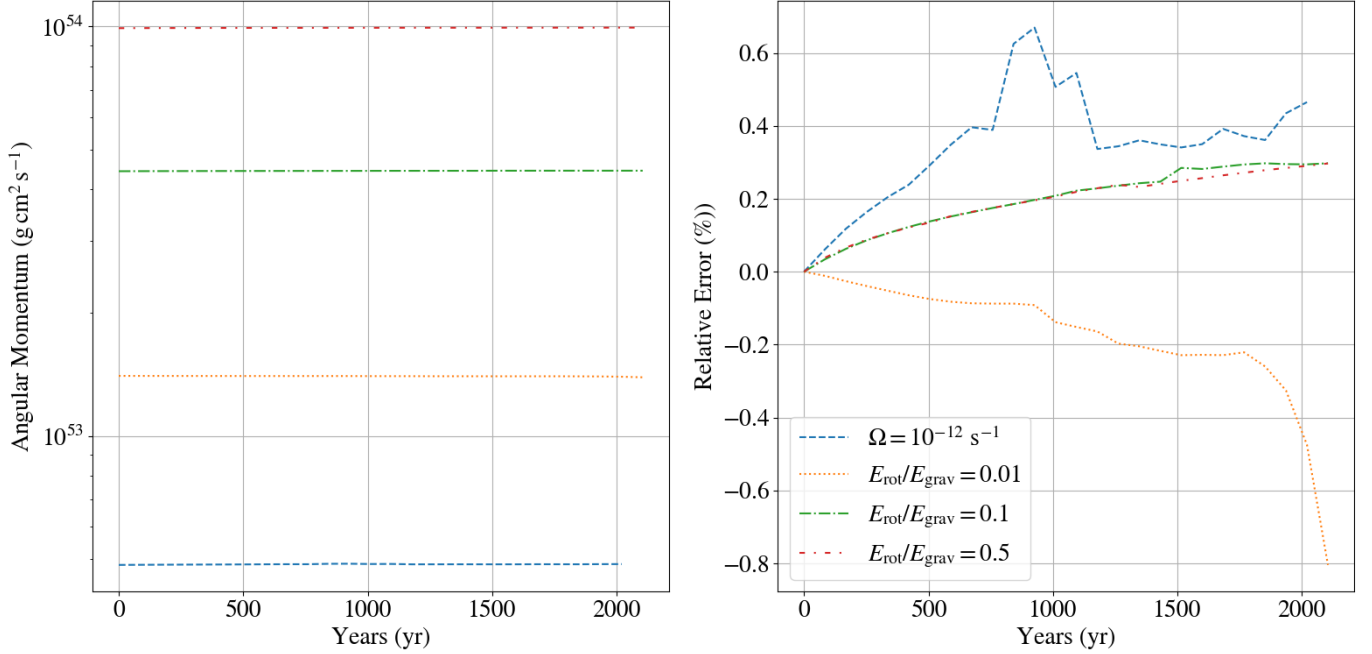
magnetic field orientation is along the  $y$ -axis in these plots. The model with  $E_{\text{mag}}/E_{\text{grav}} = 0.01$  is very weakly magnetized, and the collapse is largely spherically symmetric. However, as the magnetic field strength increases, the cloud preferentially collapses along the axis parallel to the magnetic field, resulting in a “flattening” of the cloud.

Figure 11 shows the central density as calculated from the simulations. The departure from the analytic solution becomes more pronounced as the initial  $E_{\text{mag}}/E_{\text{grav}}$  ratio increases. The evolution of



**Figure 8:** Comparisons of the analytic solution and numerical results for runs with  $E_{\text{rot}}/E_{\text{grav}} = 0.01$ ,  $0.1$ ,  $0.5$ . A run with a faster rotation deviates more from the analytic solution, which means that the collapse is slowly happening or not taking place.

the central density of the weakly-magnetized model ( $E_{\text{mag}}/E_{\text{grav}} = 0.01$ ) resembles that of the unmagnetized model with realistic heating/cooling. The moderately magnetized model ( $E_{\text{mag}}/E_{\text{grav}} = 0.1$ ) resembles the analytic solution at early times ( $t/t_{\text{ff}} \lesssim 0.9$ ), but the central density only reaches a maximal value of about  $10^{-13} \text{ g cm}^{-3}$  as the time approaches one freefall time. The strongly magnetized model ( $E_{\text{mag}}/E_{\text{grav}} = 1.0$ ) exceeds the analytic central density prior to  $t/t_{\text{ff}} \lesssim 0.6$ , but only reaches a maximum density of about  $2 \times 10^{-14} \text{ g cm}^{-3}$  by one freefall time. These results demonstrate the effect of magnetic support in resisting the global gravitational collapse of the cloud.



**Figure 9:** Conservation of the angular momentum as time passes in rotating gas cloud simulations. The angular momentum is well conserved in the simulations.

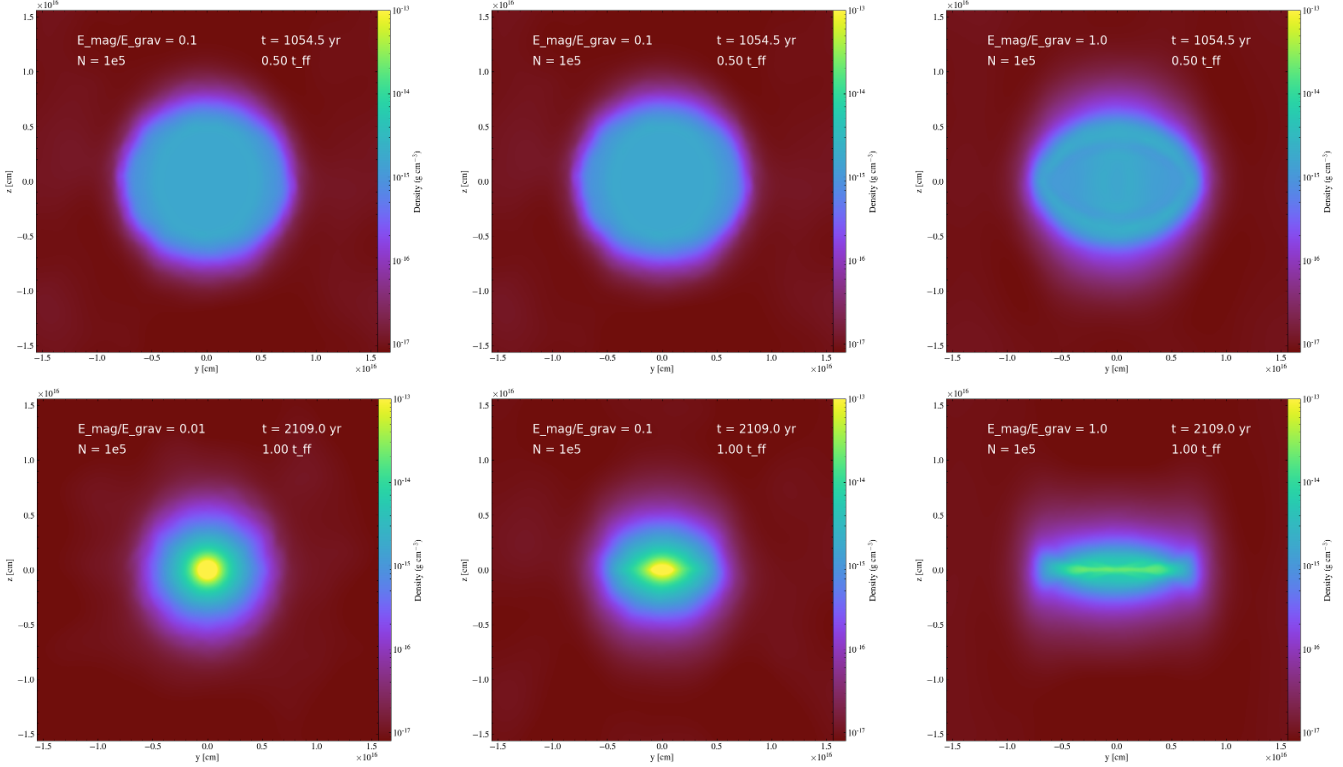


**Figure 10:** Density projection plots for static gas cloud collapse with realistic cooling/heating and ideal MHD turned on. Top row shows snapshots at  $t = 0.5 t_{\text{ff}}$ ; bottom row shows snapshots at  $t = 1 t_{\text{ff}}$ . The magnetic field is initially parallel to the  $y$ -axis of these plots. The axisymmetry of the magnetized cloud collapse is most noticeable for the model with the highest initial magnetic energy ( $E_{\text{mag}}/E_{\text{grav}} = 1.0$ ), as the collapse becomes highly flattened.

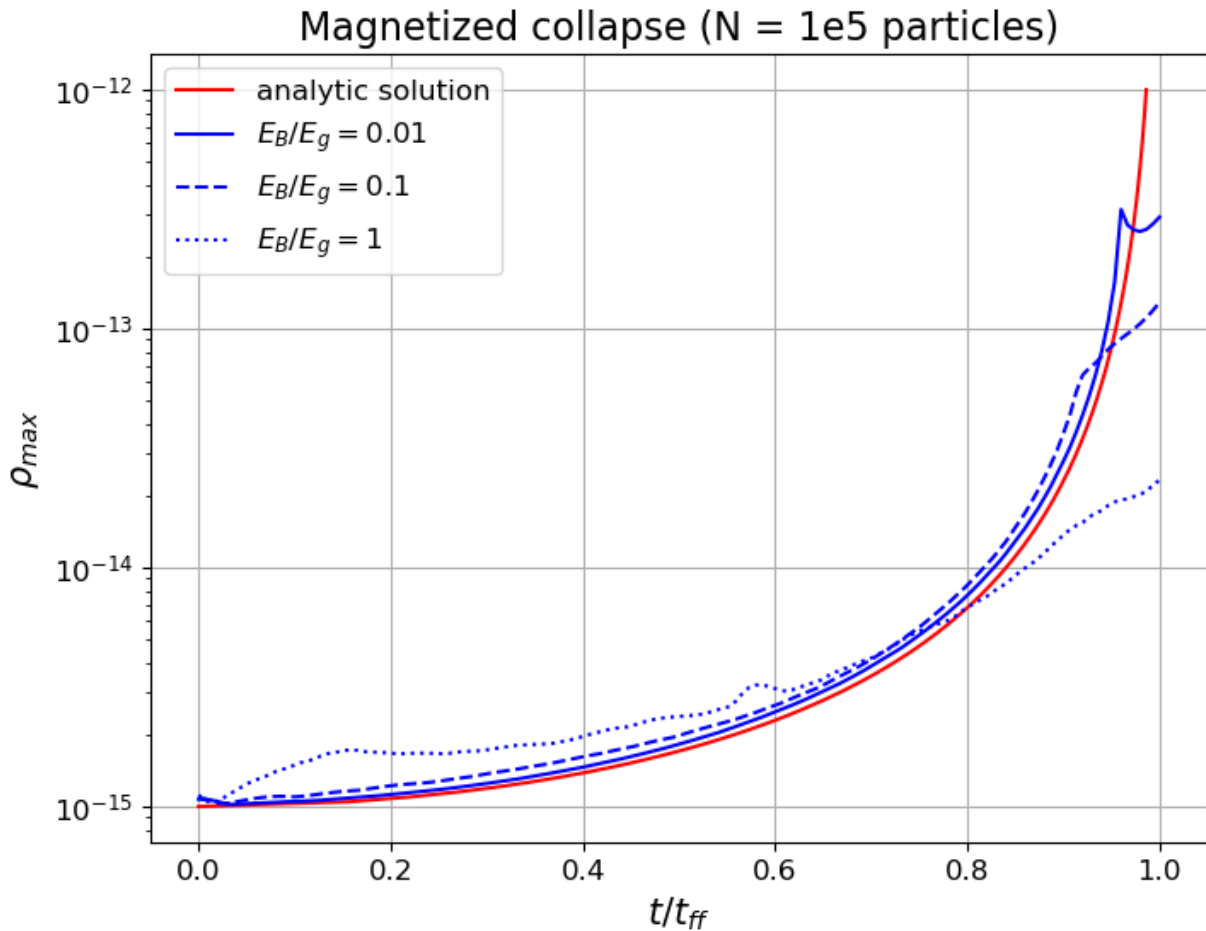


**Figure 11:** Central density comparison between analytic values calculated from Truelove et al. (1998) and simulated values calculated with GIZMO with the COOLING and MAGNETIC compile-time flags enabled. The departure from the analytic solution is most noticeable for the model with the highest initial magnetic energy ( $E_{\text{mag}}/E_{\text{grav}} = 1.0$ ).

## REFERENCES

- Grudić, M. Y., & Guszejnov, D. 2021, MakeCloud,  
1.0.  
<https://github.com/mikegrudic/MakeCloud>
- Hopkins, P. F. 2015, MNRAS, 450, 53,  
doi: [10.1093/mnras/stv195](https://doi.org/10.1093/mnras/stv195)
- Truelove, J. K., Klein, R. I., McKee, C. F., et al.  
1998, ApJ, 495, 821, doi: [10.1086/305329](https://doi.org/10.1086/305329)